Sensitivity Analysis of Junction Free Electrostatically Doped Tunnel-FET Based Biosensor

Mukesh Kumar Bind
JIIT: Jaypee Institute of Information Technology
Kaushal Nigam (kaushal.nigam@jiit.ac.in)
Jaypee Institute of Information Technology, Noida, U.P.

Research Article

Keywords: Junction Free, Polarity control, Electrostatic doping, Biosensor, Sensitivity

Posted Date: August 3rd, 2021

DOI: https://doi.org/10.21203/rs.3.rs-754761/v1

Version of Record: A version of this preprint was published at Silicon on January 6th, 2022. See the published version at https://doi.org/10.1007/s12633-021-01444-2.

Silicon manuscript No.
(will be inserted by the editor)

Sensitivity Analysis of Junction Free Electrostatically Doped Tunnel-FET Based Biosensor

Mukesh Kumar Bind · Kaushal Nigam

Received: date / Accepted: date

Abstract The electrostatic doping technique has the ability to reduce random dopant fluctuations (RDFs), fabrication complexity and high thermal budget requirement in the fabrication process of nano-scale devices. In this paper, first time propose and simulate a Junction Free Electrostatically Doped Tunnel Field-Effect Transistor (JF-ED-TFET) based biosensor for label-free biosensing applications. The gate dielectric modulation concept used for sensing the existence of biomolecules inside the nano-cavity, created in gate dielectric material towards the tunneling junction to modulate the tunneling mechanism. The sensitivity of JF-ED-TFET biosensor investigate with various types of biomolecules based on dielectric constants (k) and charge densities (ρ). The sensing response of the JF-ED-TFET biosensor analyze in terms of electric field, energy band and transfer characteristic and the sensitivity in terms of I_{ON}, I_{ON}/I_{OFF} ratio and Subtheshold Swing. The sensitivity of device investigated based on practical challenges as different filling factor and step-profile generated from the steric hinderance. The effect of temperate and nano-cavity dimensions variation on device performance also has been analyzed. In this work, various types of biomolecules as Streptavidin (k = 2.1), Ferro-cytochrome c (k = 4.7), keratin (k = 8) and Gelatin (k = 12) has been considered for the performance investigation.

Keywords Junction Free · Polarity control · Electrostatic doping · Biosensor · Sensitivity.

Kaushal Nigam (Corresponding author)
E-mail: kaushal.nigam@jiit.ac.in
Department of Electronics and Communication Engineering, Jaypee Institute of Information Technology, Noida, U.P., India

1 Introduction

The precise identity of biomolecules species and analyze their properties are very important for disease assessment and treatment. In recent decades different types of biosensors are using in various fields like medical, agriculture, food processing, environment condition monitoring [1–4] etc. Sensitivity, selectivity and fast detection timing are the basic designing parameters of biosensors. For label-free detection of biomolecules, the FET-based biosensors played a very important role due to its cost-effective manufacturing, low power consumption and scalable properties [5–8]. In 1970, the first ISFET based biosensor was proposed by P. Bergveld [9]. ISFET biosensor can detect the charge biomolecules when it present between the gate dielectric and electrolyte but ISFET biosensors can not recognized the neutral biomolecules. For avoiding ISFET biosensors limitation, dielectric modulated-FET (DM-FET) biosensors are proposed and DM-FET biosensors can detect the charged (e.g., DNA biomolecules) and non-charged (e.g.,biotin-strept-avidin) biomolecules effectively [10]. DM-FET biosensor is designed by incorporating the nano-cavity into gate dielectric material of conventional MOSFET. DM-FET based biosensor distress from low ON-current and low sensitivity issue [11]. Thereafter MOSFET-based biosensors attract the attention of researchers by the ability of high ON-current comparatively to conventional FET based biosensor [13]. The thermionic emission-based working principle, MOSFET can scale in nano regime and benefit as low power consumption and high performance. By continually narrowing the dimensions beyond the limit, the MOSFET device generates unavoidable issue as SCE (short channel effect), high OFF-state power consumption, poor control over the channel, quantum ef-

fect, low I_{ON}/I_{OFF} ratio and many others, these causes degraded performance of MOSFET-based biosensors [13]. TFET has numerous advantages over the MOSFET as work at low voltage, low power consumption, less leakage current and high-speed of operation [14–17]. By ITRS-2005, TFET becomes a futuristic device for low power applications [18]. The low ON current and ambipolar conduction (OFF-state conduction) are the main drawbacks [19] of TFET device. The low ON current considering to impediment of charge carrier movement in the silicon channel. BTBT depends on the material bandgap and effective mass of silicon material [20]. For eliminating these limitations of TFET, use some techniques as hetero material, stack gate with high k material, vertical TFET, compound material, low bandgap source material, halo doping, packet doping [21, 22]. The random dopant fluctuations (RDFs),complex fabrication process and high thermal budget requirement are critical issues of doped devices [23]. The charge plasma and electrostatic doping are the new concepts who eliminate these limitations from the fabrication process [24]. Using these techniques mass production, cost-effective and reliable TFET device manufacturing become possible easily [25, 26]. In this paper, a junction-free electrically doped tunnel field-effect transistor (JF-ED-TFET) based biosensor is proposed for label-free identification of biomolecules. By using an electrostatic doping technique the device becomes cost-effective and scaled-down without degrade its performance [27]. To achieve the high sensitivity, the nano-cavity creates near to source-channel interface junction of device. For the performance investigation, target biomolecules consider as neutral and charged with different dielectric constants (k) and charge densities (ρ) (positive and negative). The neutral biomolecules can be identifying based on their own dielectric constant and charged biomolecules can be detected based on their charge density and dielectric constant also. For sensitivity analysis, consider the air ($k = 1$) as reference biomolecules and compare with other biomolecules of different dielectric constant ($k > 1$) and charge density ρ. The sensitivity of the JF-ED-TFET biosensor is proportional to drain current (I_{DS}) and drain current (I_{DS}) is directly proportional to changes of the biomolecules dielectric constants (k) as well as charge densities (ρ).

2 2-D Structure and design Parameters of proposed biosensor

The proposed device JF-ED-TFET biosensor schematic view of the 2-D structure shown in Fig. (1) and designing parameters are given in table-1. Apply electrostatic doping concept to convert the device from n-n-n (device region-drain, channel and source) to device n^+-i-p^+ (TFET) [27], apply appropriate biases supply at PGs, as at PG-1 positive bias (+1.2 V) and at PG-2 negative bias (-1.2 V). Consider the metal work function of polarity gates and control gate are similar to 4.5 eV. For the drain/source contact use Nickel Silicide (NiSi) with barrier potential of 0.45 eV [27]. Spacer gap at drain-channel junction (D_{gap}) consider 8 nm

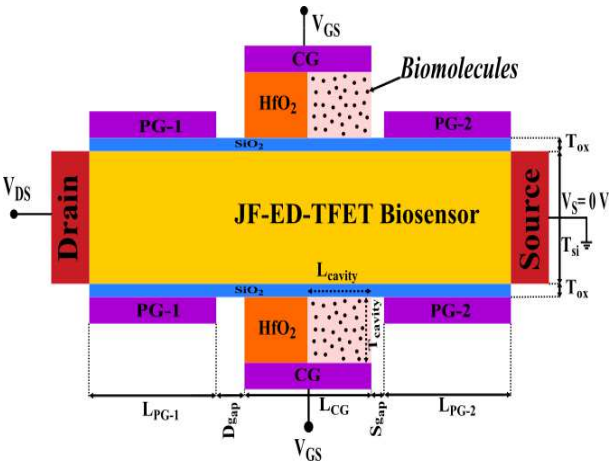

Fig. 1: 2-D cross-sectional view of JF-ED-TFET biosensor.

Table 1: Designing parameters of JF-ED-TFET biosensor used in simulation.

Design Parameters	Symbol	Value
Silicon layer thickness	T_{si}	10.00 nm
SiO_2 thickness	T_{ox}	0.50 nm
HfO_2 thickness	T_{HfO_2}	5.50 nm
Length of CG	L_{CG}	50.00 nm
Length of PG-1	L_{PG-1}	50.00 nm
Length of CG-2	L_{PG-2}	50.00 nm
Cavity length	L_{Cavity}	25.00 nm
Cavity thickness	T_{Cavity}	5.50 nm
Metal workfunction of all Gates	ϕ_g	4.5 eV
Source-Gate spacer	S_{gap}	2.00 nm
Drain-Gate spacer	D_{gap}	8.00 nm
Silicon layer concentration	*n-type*	1e15 cm^{-3}

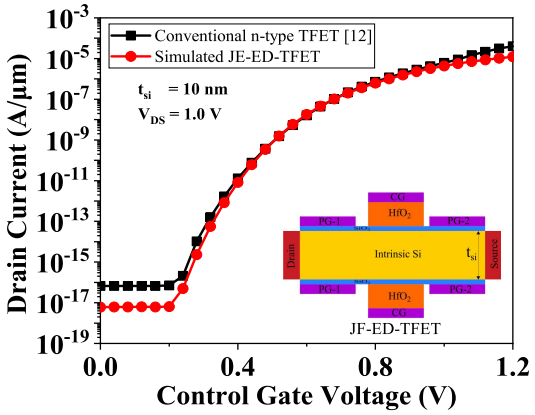

Fig. 2: I_D-V_{CG} characteristic of propose device JF-ED-TFET calibrated with conventional doping less TFET [12].

Table 2: The sensitivity of proposed biosensor with various dielectric constants and charge densities.

Employed Biomolecules	**Dielectric Constant** (k)	**Charge Density** (ρ)	**Sensitivity** (V_{DS} = 1.0 V, and V_{GS} = 1.2 V)
Neutral Biomolecules	2.1		1.24x10^4
	4.7		1.41x10^8
	8		1.20x10^{10}
	12		1.12x10^{11}
Positive Charged Biomolecules	8	ρ = 1x10^{11} C/cm^2	1.32x10^{10}
		ρ = 5x10^{11} C/cm^2	2.14x10^{10}
		ρ = 1x10^{12} C/cm^2	3.64x10^{10}
Negative Charged Biomolecules	8	ρ = -1x10^{11} C/cm^2	1.01x10^{10}
		ρ = -5x10^{11} C/cm^2	5.61x10^9
		ρ = -1x10^{12} C/cm^2	2.44x10^9

for reducing the ambipolar conduction and source-channel junction (S_{gap}) consider 2 nm to increase the drain current. Based on physical dimensions of biomolecules consider the nano-cavity height as 5.5 nm [28, 29]. During simulation various kinds of biomolecules such as Strepatvidin (k = 2.1), Ferro-cytochrome c (k = 4.7), Keratin (k = 8) and Gelatin (k = 12) with different dielectric constant as well as charge density are use for investigate the sensing performance of JF-ED-TFET biosensor.

3 Propose Device Modulation and Calibration

Silvaco ATLAS TCAD device simulator tool, version V5.0.10 R [30] is use for simulation of the JF-ED-TFET biosensor. The JF-ED-TFET biosensor work based on the band to band tunneling (BTBT) so nonlocal BTBT model used to account of tunneling rate. Universal Schottky Tunneling (UST) model use for NiSi drain/source contact. The SRH (Shockley-Read-Hall) model used for concentration-dependent carrier recombination and Auger model are also incorporated. For the account of carrier mobility, Fermi-Dirac statistic and field-dependent mobility models are used. Wentzel-Kramers-Brillouin method has been employed for numerical tunneling. TAT model is also incorporated for process-dependent issues in simulation. For result accuracy at device interface layers and at tunneling region a very dense meshing has been designed.
For device calibration, The transfer characteristic of proposed device calibrated with conventional doping-less TFET [12] and observed it is also replica of [12] shown in Fig. 2.

4 Results and Discussion

4.1 Impact of Biomolecules Properties on Device Characteristics

The variations of JF-ED-TFET biosensor characteristics due to immobilization of biomolecules in nano-cavity region with different dielectric constants and charge densities have studied in this section. Here consider the biomolecules dielectric constants (k) as 1, 2.1, 4.7, 8 and 12, and the charge densities as $\pm$1x10^{11}, $\pm$5x10^{11}, and $\pm$1x10^{12} C/cm^2 for performance investigation of JF-ED-TFET biosensor.

4.1.1 Effect on Electric Field

The internal electric field variations of JF-ED-TFET biosensor with neutral biomolecules shown Fig. 3(a), observed when increase the dielectric constant of biomol-ecules, the electric field at tunneling junction increase. The high electric field at tunneling junction, minimize the tunneling width hence drain current of the device increased. For dielectric constant k = 12 the peak electric field can 3.4x10^6 V/cm obtained from proposed model. The electric field increase (decrease) with increment of positive (negative) charge density of biomolecules due to more negative (positive) charge carriers induce in channel region hence potential difference between source-channel increase (decrease) hence

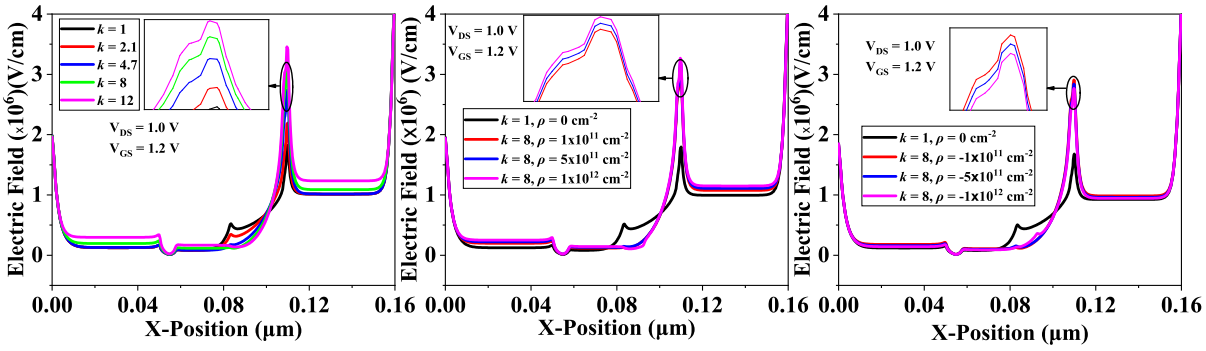

(a) (b) (c)

Fig. 3: Electric field variation along x-axis with varying (a) Dielectric constants (k) at $\rho = 0$ (b) Positive charge densities (ρ) at $k = 8$ (c) Negative charge densities (ρ) at $k = 8$.

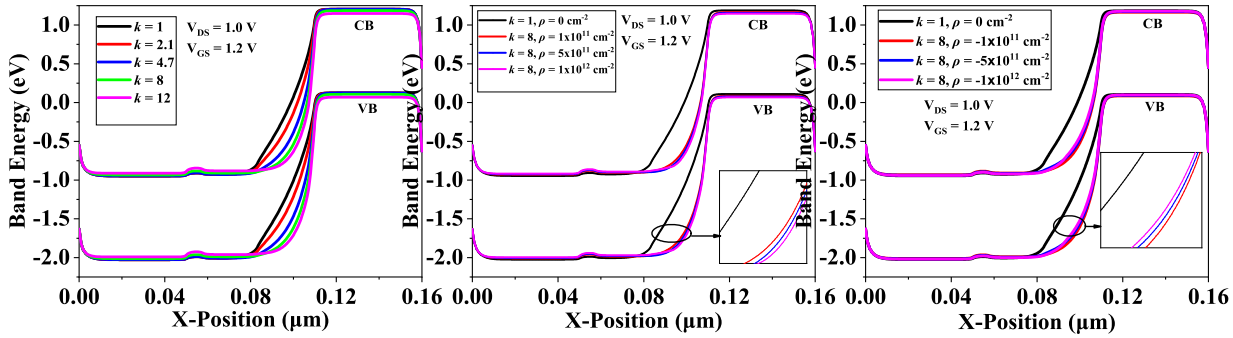

(a) (b) (c)

Fig. 4: Variation of Energy band along x-axis with varying (a) Dielectric constants (k) at $\rho = 0$ (b) Postive charge densities (ρ) at $k = 8$ (c) Negative charge densities (ρ) at $k = 8$.

electric field increase (decrease) at junction. The electric field variation with positive and negative charge density respectively shown in Fig. 3(b)-(c).

4.1.2 Effect on Energy Band

The energy band profile of proposed biosensor with various dielectric constants (k) and charge densities (ρ) shown in Fig. 4(a)-(c). It can be seen, when the dielectric constant of neutral biomolecules increase, the band-gap decrease at tunneling junction hence tunneling probability of charge carrier increase shown in Fig. 4(a). With dielectric constant $k = 12$, the band gap is very low as compare to dielectric constant $k = 1$, hence charge tunneling probability is very high at $k = 12$. Fig. 4(b) and Fig. 4(c) illustrate the impact on band bending at the tunneling junction, in presence of different charge densities at the Si-SiO_2 interface. It can be seen with positive charge density band-gap decrease and tunneling probability increase, while in case of negative charge density band-gap increase.

4.1.3 Impact on Drain Current

The I_D-V_{GS} characteristic of JF-PE-TFET biosensor with various dielectric constants (k) of neutral biomolecules ($\rho = 0$) shown in Fig. 5(a). Observed, by increasing the dielectric constant, the drain current of device increase and threshold voltage (V_{Th}) decrease because increased effective gate capacitance of device. Fig. 5(b) shows the I_D-V_{GS} plot with charged biomolecules of fixed dielectric constant $k = 8$ and observed by increasing the negative charge density the drain current decrease but with positive charge density it increases. This phenomenon understood with the voltage balance equation of MOSFET [31] given as:

$$V_{GS} = \psi_S + \phi_{MS} - \left(\frac{q.N_{bio}}{C_{ox'}}\right) \tag{1}$$

where

$$C_{ox'} = k/t_{ox}$$

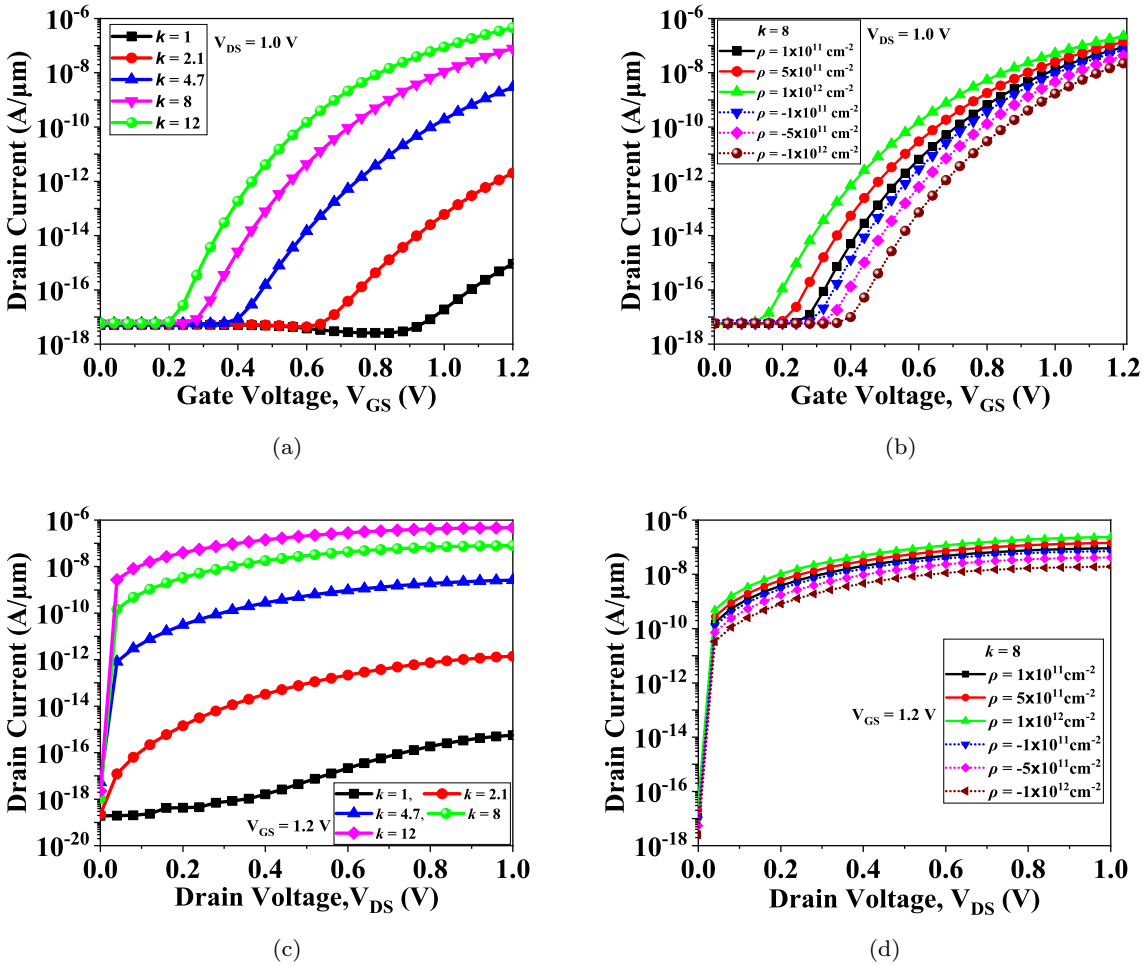

Fig. 5: I_{DS}-V_{GS} characteristic of proposed biosensor with various (a) Dielectric constants (k) at $\rho = 0$, (b) Ccharge densities (ρ) at $k = 8$; and I_{DS}-V_{DS} characteristic of proposed biosensor with various (c) Dielectric constant (k) at $\rho = 0$ and (d) Charge densities (ρ) at $k = 8$.

in equation (1) V_G, ψ_S, ϕ_{MS}, N_{bio}, q, k and t_{ox} are representing gate voltage, surface potential, contact potential, biomolecules charge per unit area, electron charge, dielectric constant and oxide thickness respectively. During device simulation, gate voltage is constant at applied voltage, but surface potential decreasing by increasing of negative charge density from equation (1), the gate voltage of device decrease hence drain current decrease but with positive charge density surface potential increase hence drain current increase. The JF-ED-TFET biosensor out-put characteristic I_D-V_{DS} plotted at constant V_{GS} with various dielectric constants (k) and charge densities (ρ) shows in Fig. 5(c)-(d) and notice that its present similar behavior shown in above Fig. 5(a)-(b).

4.2 Sensitivity Analysis

Sensitivity is a very important parameter of any type of sensor and high sensitivity is desirable. JF-ED-TFET biosensor sensitivity analyze in terms of drain current ($S_{I_{DS}}$), subthreshold swing (S_{SS}) and I_{ON}/I_{OFF} ratio. The drain current sensitivity ($S_{I_{DS}}$) is define as [32]:

$$S_{I_{DS}} = \left(\frac{I_{DS}^{bio} - I_{DS}^{air}}{I_{DS}^{air}} \right) \tag{2}$$

here, I_{DS}^{bio} and I_{DS}^{air} are the drain currents when nano-cavity filled with biomolecules (k ¿1) and air($k = 1$). Fig. 6(a)-(b) shows the JF-ED-TFET biosensor current sensitivity ($S_{I_{DS}}$) along V_{GS} with different dielectric constants (k) and charge densities (ρ). It is observed that when increase the dielectric constants (k) the sensitivity of device increase and similarly with positive charge densities due to increasing the I_{ON} current of device.

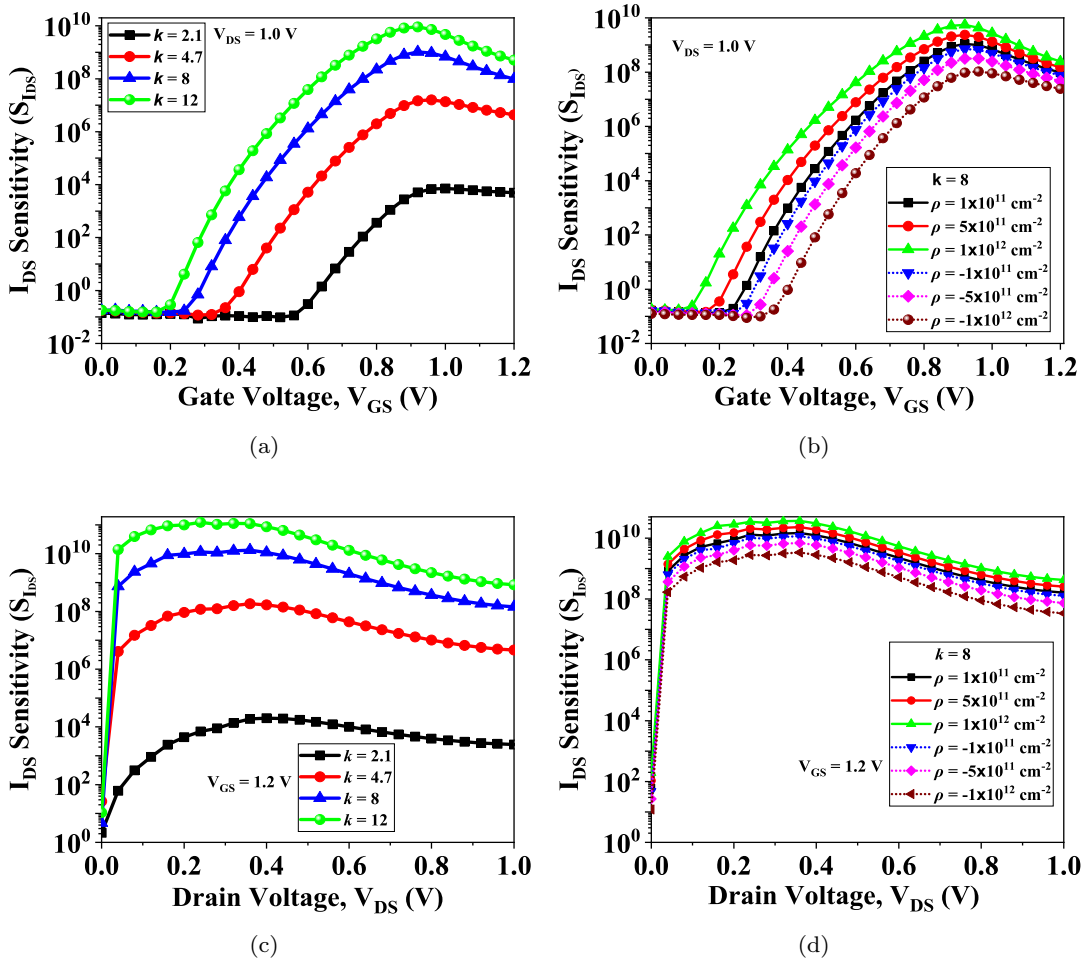

Fig. 6: I_{DS} sensitivity of JF-ED-TFET biosensor along V_{GS} with different (a) Dielectric constants (k) at $\rho = 0$, (b) Charge densities (ρ) at $k = 8$; and I_{DS} sensitivity of JF-ED-TFET biosensor along V_{DS} with differents (c) Dielectric constants (k) at $\rho = 0$, (d) Charge densities (ρ) at $k = 8$.

But with negative charge density the I_{ON} current decrease hence the sensitivity of device decrease. Fig.6(c)-(d) shows the drain current sensitivity ($S_{I_{DS}}$) vs drain voltage (V_{DS}) plot with different dielectric constants (k) and charge densities (ρ, observed the device offer high sensitivity $S_{I_{DS}}$) at lower drain voltage.

The reflection of charge and neutral biomolecules with different dielectric constant on sensitivity of the JF-ED-TFET biosensor mentioned in table-2. The propose biosensor sensitivity increase with increase the dielectric constant as well as positive charge density due to increment of drain current but in case negative charge density the sensitivity of biosensor decrease due to decrements of drain current.

The sensitivity of JF-ED-TFET biosensor can be analyzed in term of I_{ON}/I_{OFF} ratio and calculated as:

$$S_{I_{ON}/I_{OFF}} = \left(\frac{(I_{ON}/I_{OFF})^{bio} - (I_{ON}/I_{OFF})^{air}}{(I_{ON}/I_{OFF})^{air}} \right) \quad (3)$$

Fig. 7(a)-(b) depicted the increment I_{ON}/I_{OFF} sensitivity of JF-ED-TFE biosensor with increasing the dielectric constant and positive charge density of biomolecules because tunneling barrier width between valance band (VB) of source and conduction band (CB) of channel start decreasing hence drain current (I_{DS})of device increase. but I_{ON}/I_{OFF} sensitivity shows adverse behavior with increment of negative charge density (ρ), depicted in Fig.7(c). The TFET, become a futuristic device for low power applications because TFET offer low soubthershold swing (<60 mV/decade) and low OFF-current. The JF-ED-TFET biosensor offer low subthershole swing (SS) as 27.2 mV/decade hence it efficiently work at low voltage and detect the biomolecules within limited time. The Subthreshold swing (SS) [41] and SS sensitivity of the JF-ED-TFET biosen-

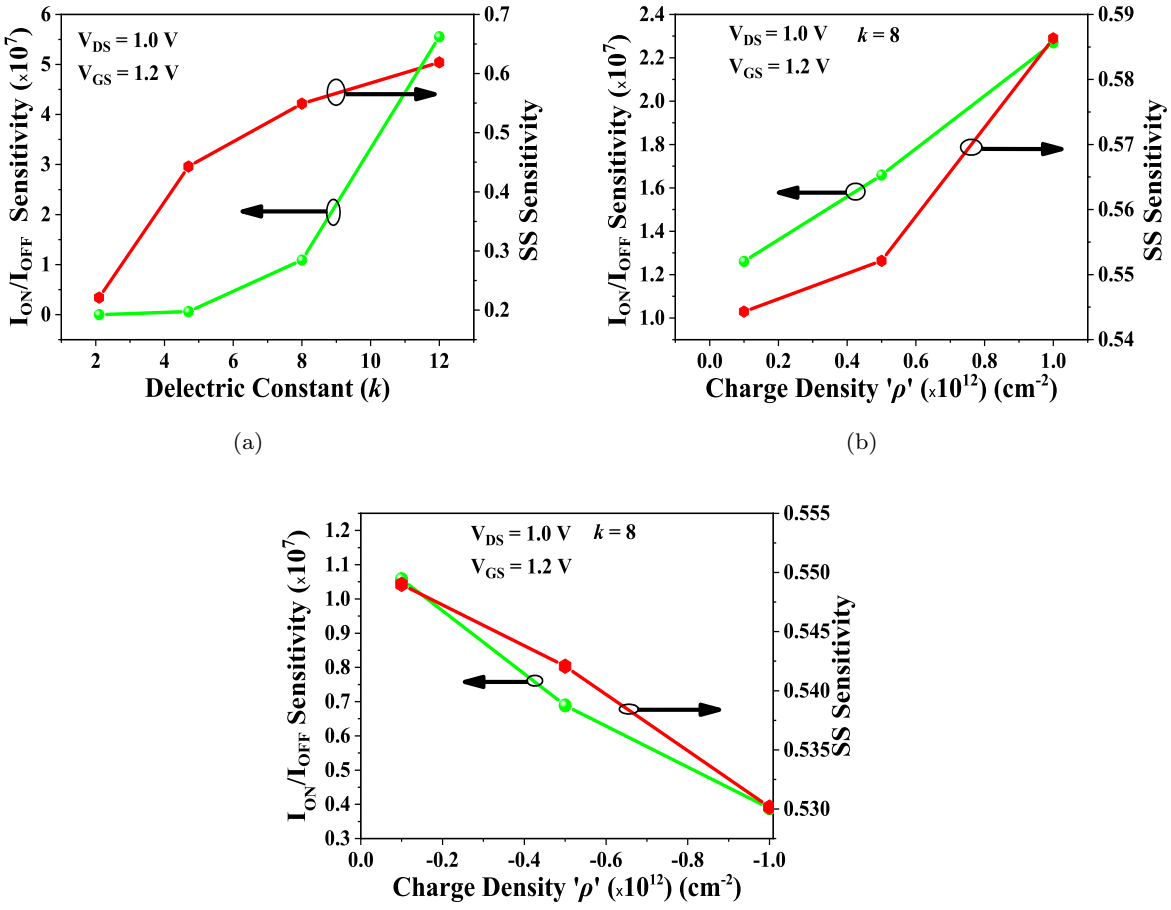

Fig. 7: Variation of I_{ON}/I_{OFF} and SS sensitivity with different (a) Dielectric constants (k) at $\rho = 0$, (b) Positive charge densities (ρ) at $k = 8$ and (c) Negative charge densities (ρ) at $k = 8$.

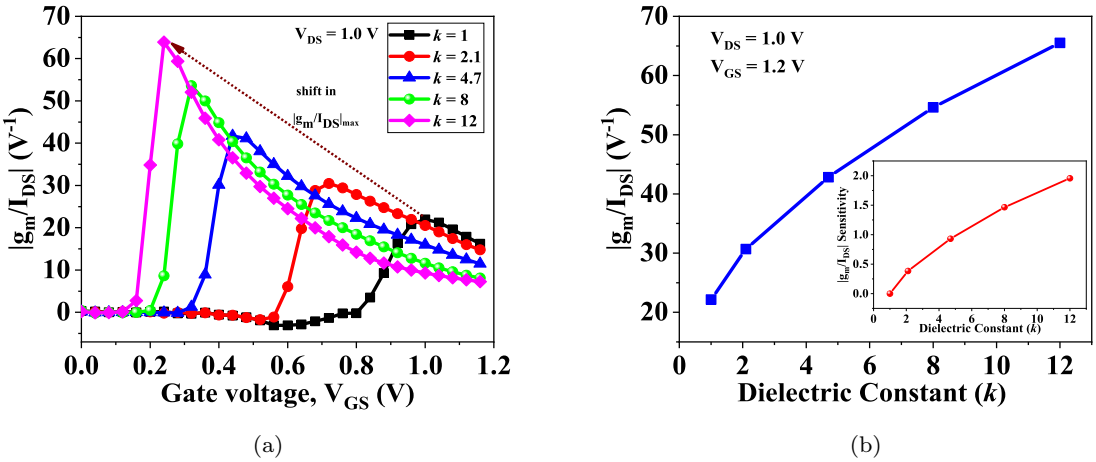

Fig. 8: (a) g_m/I_{DS} plot along V_{GS} and (b) variation of g_m/I_{DS} values and g_m/I_{DS} sensitivity (inset), for different dielectric constants (k) at $\rho = 0$.

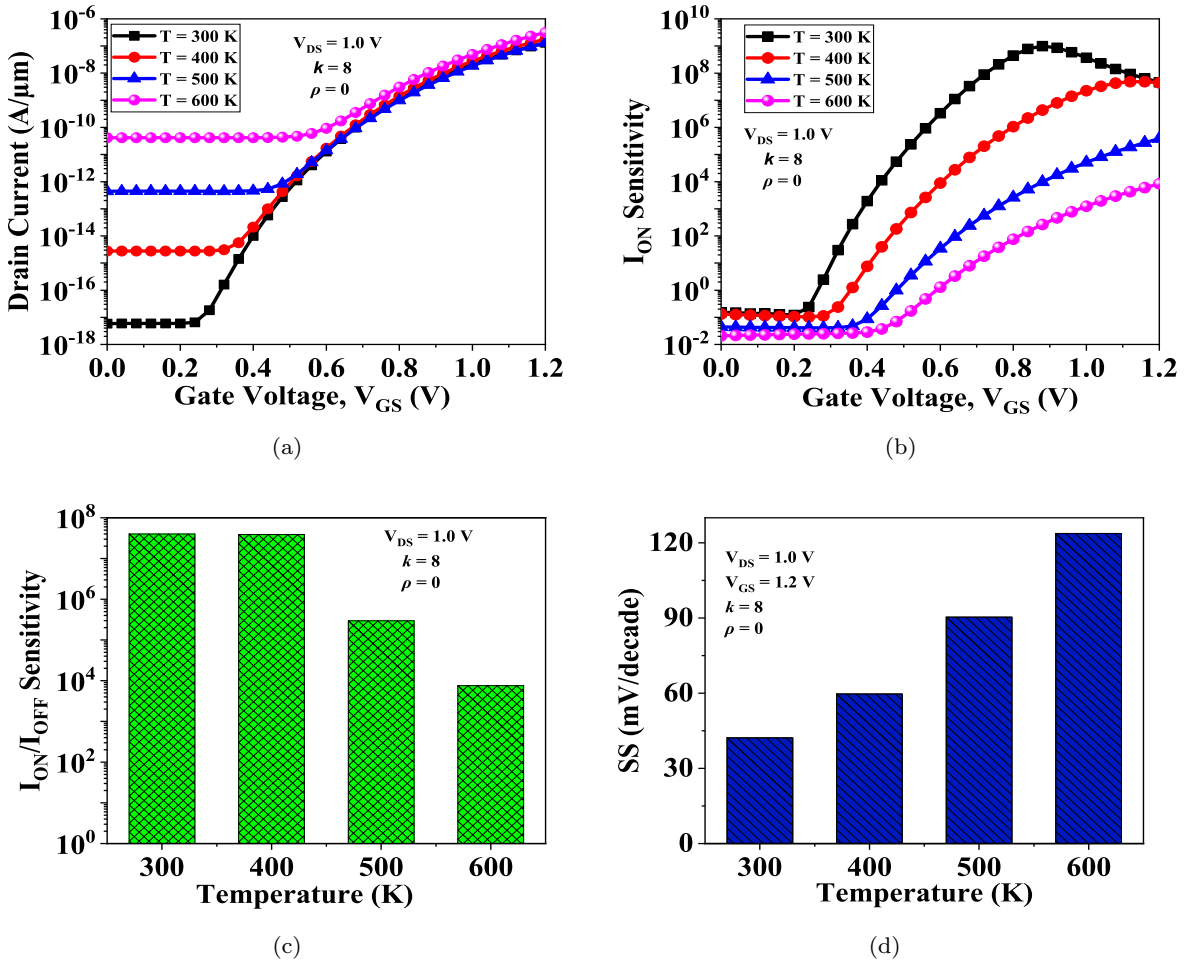

Fig. 9: (a) Transfer characteristic of JF-ED-TFET biosensor and (b) I_{ON} Sensitivity, at $k = 8$ for different temperature

sor evaluated [33] as:

$$SS = \left(\frac{\delta V_{GS}}{\delta log I_{DS}}\right)(mV/decade) \tag{4}$$

and

$$S_{SS} = \left(\frac{SS_{(air)} - SS_{(bio)}}{SS_{(air)}}\right) \tag{5}$$

The SS sensitivity variation of proposed biosensor with different dielectric constants (k) and charges density (ρ) shown in Fig. 7(a)-(c) respectively. From figure observed, SS sensitivity increase by increasing the dielectric constants (k) and positive charge density (ρ), whereas SS sensitivity decrease with increasing the negative charge densities.

The Transconductance-to-current ratio (g_m/I_{DS}) is a sensing metric [34] for better sensitivity and selectivity of neutral biomolecules. The $|g_m/I_{DS}|$ of JF-ED-TFET biosensor has been plotted against gate voltage with different dielectric constant shown in Fig 8(a). From figure observed that when the dielectric constant increase the device offers a higher $|g_m/I_{DS}|$ value at lower drain current. The increment in $|g_m/I_{DS}|$ value and $|g_m/I_{DS}|$ sensitivity with increment the dielectric constant of biomolecules shown in Fig. 8(b). The g_m/I_{DS} values are obtained as [34]:

$$|g_m/I_{DS}| = \frac{ln(10)}{SS}(V^{-1}) \tag{6}$$

4.2.1 Impact of temperature variation on sensitivity

Fig. 9(a)-(b) depict the change in device transfer characteristic and I_{ON} sensitivity due to temperature variation. It can be seen that when the temperature increase the OFF-state current increase but ON-current slightly change because ON-current depends on BTBT Tunneling rather than the temperature variation. The I_{ON} sensitivity of JF-ED-TFET biosensor decrease because the drain current with empty cavity ($k = 1$) increase by increasing the temperature, shown in Fig.9(b). The

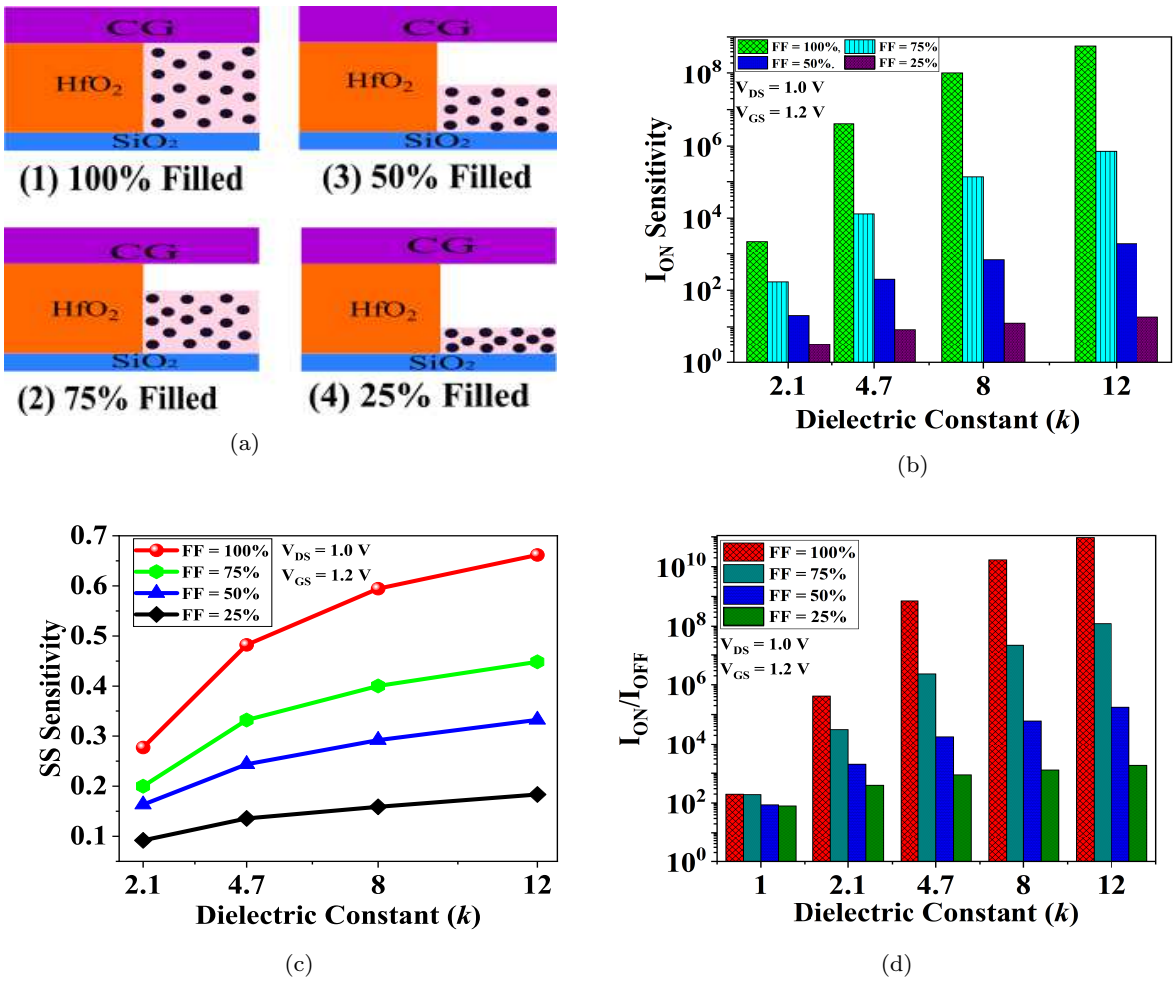

Fig. 10: (a) Four different assumptions for nano-cavity filled by target biomolecules, (b) I_{ON} sensitivity, (c) SS sensitivity and (d) I_{ON}/I_{OFF} ratio, along different dielectric constant for different Fill Factor (FF).

Table 3: Comparison of Sensitivity Values with Refreshes

References	Dielectric constant (k)	Approximate Sensitivity
[31]		1.31x10^8
[37]		5.45x10^9
[38]	$k = 12$	4.75x10^5
[39]		1.04x10^6
[40]		1.7x10^8
[41]		1.73x10^{10}
Proposed	”	1.12x10^{11}
[42]	$k = 8$	2.6x10^5
Proposed		1.20x10^{10}
[10]	$k = 2.1$	1.00x10^4
Proposed		1.24x10^4

I_{ON}/I_{OFF} sensitivity of JF-ED-TFET biosensor shown in Fig. 9(c). The I_{ON}/I_{OFF} sensitivity decrease with increasing the temperature because the OFF-state current increase by increasing the temperature. The shubthreshold swing increase with increasing the temperature shown in Fig. 9(d).
The sensitivity values obtained by propose JF-ED-TFET biosensor with different dielectric constants are compare with various previous reported works given in table-3 and observed the JF-ED-TFET biosensor obtained high 1.12x10^{11} sensitivity with neutral biomolecules of dielectric constant $k = 12$.

4.3 Considering non-ideal issues

The challenge facing during realistic use of biosensor, it is necessary investigate performance of biosensor with different fill factor (FF). Fill factoe (FF) defines as:

$$FF\% = \frac{A_{cavity}^{bio}}{A_{cavity}^{total}}.100 \tag{7}$$

Here A_{cavity}^{bio} is area occupied by target biomolecules and A_{cavity}^{total} is total area of cavity [35]. In this work,

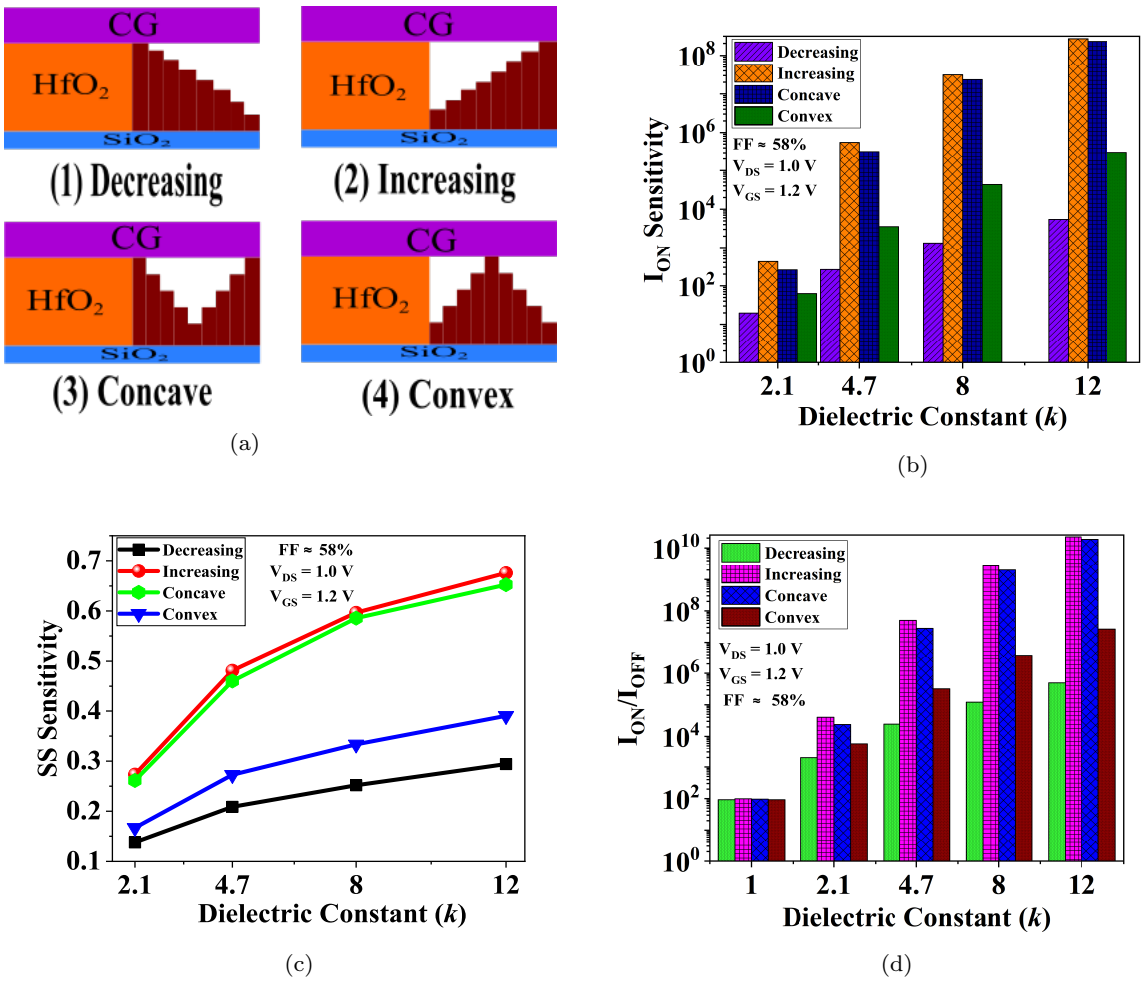

Fig. 11: (a) Partial filled nano-cavity with different step profile, (b) I_{ON} sensitivity, (c) SS Sensitivity and (d) I_{ON}/I_{OFF} ratio , along different dielectric constant for different step profile with FF ≈ 58%.

discussed four possible FF as 25%, 50%, 75% and 100% depicted in Fig. 10(a). I_{ON} sensitivity along with different FF and dielectric constant shows in Fig. 10(b) and observed when fill factor (FF) increase, the JF-ED-TFET biosensor I_{ON} sensitivity increase. Fig. 10(c)-(d) shows the SS sensitivity and I_{ON}/I_{OFF} ratio with varying dielectric constant and FF, here observed that the sensitivity of JF-ED-TFET biosensor improved by increasing the FF as well as the dielectric constant of biomolecules.

The JF-ED-TFET biosensor simulated in presence of steric hindrance to understanding the practical challenge. Here considering four varying step profiles as decreasing, increasing, concave and convex with filling factor of ≈ 58%, this arrangement illustrated in Fig. 11(a). The I_{ON} sensitivity along with different dielectric constant and step profile depicted in Fig. 11(b) and observe, the high sensitivity draw with Increasing and concave step profile because in these two step profile got highest proximity of target biomolecules at source-channel interface, hence tunneling barrier decrease with these step profile [36]. Similarly the SS sensitivity and the I_{ON}/I_{OFF} ratio are high with increasing and concave step profile as compare to decreasing and convex step profile shown in Fig.11(c)-(d).

4.4 Effect of nano-cavity geometry variations

The effect of cavity dimension variations on the performance of biosensor has been investigated by simulation with two measure constraints as cavity length (L_{cavity}) and cavity thickness (T_{cavity}). The I_{DS}-V_{GS} characteristic of JF-ED-TFET biosensor with neutral biomolecule ($k = 8$) shown in Fig. 12(a). It can be seen that very less impact of L_{cavity} variations on the drain current because propose device works based on BTBT tunneling phenomenon. From Fig.12(b) observed, the I_{ON} sensitivity increase with increasing the cavity length because drain current of device decrease with empty cavity by increment of cavity length. The effect of

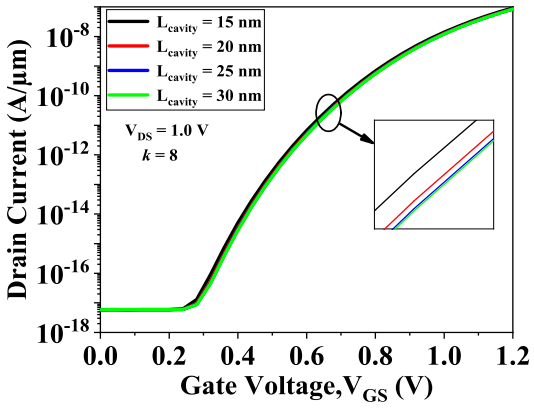

(a)

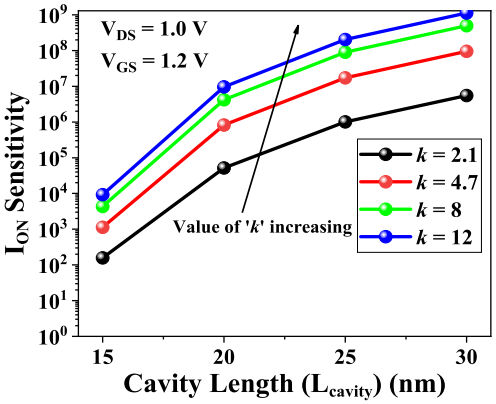

(b)

Fig. 12: (a) Transfer characteristic of JF-ED-TFET biosensor and (b) I_{ON} Sensitivity, with varying cavity length (L_{cavity}) at $k = 8$.

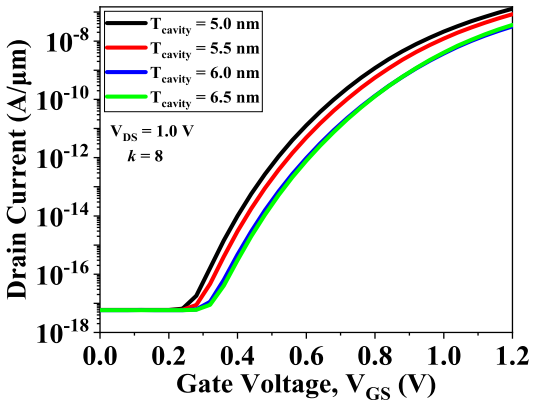

(a)

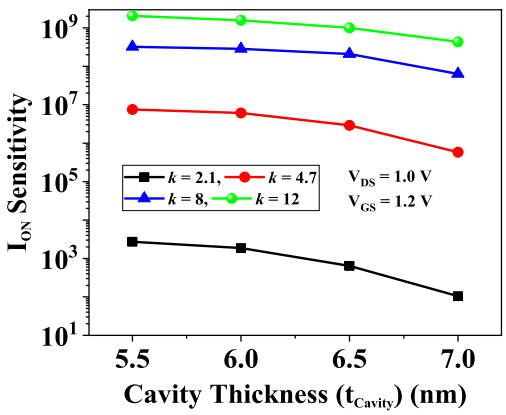

(b)

Fig. 13: (a) Transfer characteristic of JF-ED-TFET biosensor and (b) I_{ON} Sensitivity, with varying cavity length (T_{cavity}) at $k = 8$.

variation in cavity thickness (T_{cavty}) on the I_{ON} sensitivity of JF-ED-TFET biosensor illustrated in Fig.13(b) and observed, by increasing the cavity thickness (T_{cavity}) the sensitivity of device decrease because decrease the drain current, shown in Fig. 13(a), due to decreasing the effective gate capacitance of device.

5 Conclusion

In this paper, the sensing performance of nanocavity embedded dielectric modulated JF-ED-TFET biosensor investigated for label-free detection of biomolecules. Analyze results shows that the JF-ED-TFET biosensor can be used for intuitive examination for charged or neutral biomolecules with different dielectric constant. The electrostatic doping concept offer to less fabrication complexity, low cost and reliable device against RDFs. The effect of neutral and charged biomolecules on the electrical parameters of JF-ED-TFET biosensor as electric field, energy band, transfer characteristic, subthreshold swing (SS) and I_{ON}/I_{OFF} ratio have been studies. The simulated results as peak drain current (I_{DS}) is 8.55x10^{-6} A/μm, Electric field is 3.70x10^{6} V/cm, steeper subthreshold swing (SS) is 27.2 mV/decade (< theoretical limit as 60 mV/decade), I_{ON}/I_{OFF} ratio is 2.81x10^{11} and g_m/I_{DS} value is 67 (> theoretical limit 38.4) obtained from this proposed model. The JF-ED-TFET biosensor offer high drain current sensitivity is 1.12x10^{11} and I_{ON}/I_{OFF} sensitivity is 5.74x10^{7}, SS sensitivity is 0.65 and g_m/I_{DS} sensitivity is 1.8 for neutral biomolecules with dielectric constant *'k'* = 12. For validate the realistic approach of JF-ED-TFET biosensor have been consider the irregular arrangement of biomolecules filled (step profile) in cavity and different fill factors in simulation. The device design parameters optimizes for high sensitivity, hence the proposed device JF-PE-TFET becomes an advantageous device in the field of biosensing appli-

cations.

Declarations

Acknowledgements
The authors would like to thank the Department of Electronics and Communication Engineering, Jaypee Institute of Information Technology, Noida, Uttar Pradesh, India, for providing us the computational facilities.

Author contributions:
1. Kaushal Nigam - Concept and methodology
2. Mukesh Kumar Bind - Resource, simulation

Consent for Publication Yes.
Consent to Participate Yes.
Availability of Data and Material: The data and material concerned to the manuscript may be made available on request.
Funding: Not applicable
Compliance with Ethical Standards
The manuscript follows all the ethical standards, including plagiarism.
Conflict of Interests: No conflicts of interest.
Research involving human participants and/or animals: This article does not contain any studies with human participants or animals performed by any of the authors
Informed consent: Informed consent was obtained from all individual participants included in the study.

References

1. Malhotra BD, Kumar S, Pandey CM (2016) Nanomaterials based biosensors for cancer biomarker detection. *J Phys Conf Ser* 704:1–11. https://iopscience.iop.org/article/10.1088/1742-6596/704/1/012011.
2. Kim S et al (20120 A transistor-based biosensor for the extraction of physical properties from biomolecules. *Appl Phys Lett* 101:073703.https://doi.org/10.1063/1.4745769.
3. Shin J, Choi S, Yang JS, Jung HI, Jung AI (2017) Smart forensic phone: Colorimetric analysis of a bloodstain for age estimation using a smartphone. *Sens Actuators B Chem* 243:221–225. https://doi.org/10.1016/j.snb.2016.11.142.
4. Nguyen VT, Kwon YS, Gu MB (2017) Aptamer-based environmental biosensors for small molecule contaminants. *Current Opinion Biotechnol* 45:15–23. https://doi.org/10.1016/j.copbio.2016.11.020
5. Seabaugh AC, Zhang Q (2010) Low-voltage tunnel transistors for beyond CMOS logic. *Proc IEEE* 98:2095–2110. https://ieeexplore.ieee.org/document/5608485
6. Choi WY, Park BG, Lee JD, King Liu TJ (2007) Tunneling field-effect transistors (TFETs) with subthreshold swing (SS) less than 60 mV/dec. *IEEE Electron Device Lett* 28:743–745.https://ieeexplore.ieee.org/document/-4278352
7. Wang PF et al (2004) Complementary tunneling transistor for low power application. *Solid-State Electron* 48:2281–2286. https://doi.org/10.1016/j.sse.2004.04.006
8. Ionescu AM, Riel H (2011) Tunnel field-effect transistors as energyefficient electronic switches. *Nature* 479:329–337.https://doi.org/10.1038/nature10679
9. Bergveld P (1970) Development of an ion-sensitive solid-state device for neurophysiological measurements. *IEEE Trans Biomed Eng* 17:70–71. https://ieeexplore.ieee.org/document/4502688
10. Im H, Huang XJ, Gu B, Choi YK (2007) A dielectric-modulated field-effect transistor for biosensing. *Nature Nanotechnol* 2:430–434. https://doi.org/nnano.2007.180
11. Anvarifard MK, Ramezani Z, Amiri IS (2021)High Ability of a Reliable Novel TFET-Based Device in Detection of Biomolecule Specifies-A Comprehensive Analysis on Sensing Performance. *IEEE sensors J* 21:5. https://doi.org/document/9291463
12. Boucart K, Ionescu AM (2007) Double-gate tunnel FET with high-k gate dielectric. *IEEE Trans. Electron Devices* 54:1725–1733. https://doi.org/10.1109/TED.2007.899389
13. Shreya S, Khan AH, Anand S (2020)Core-Shell Junctionless Nanotube Tunnel Field Effect Transistor: Design and Sensitivity Analysis for Biosensing Application. *IEEE sensor J* 20:2. https://doi.org/10.1109/JSEN.2019.2944885.
14. Koswatta SO, Lundstrom MS, Nikonov DE (2009) Performance comparison between p-i-n tunneling transistors and conventional MOSFETs. *IEEE Trans. Electron Devices* 56:456–465. https://doi.org/10.1109/TED.2008.2011934.
15. Colinge JP et al (2010) Nanowire transistors without junctions. *Nature Nanotechnol* 5:225–229. https://doi.org/10.1038/nnano.2010.15.
16. Bhuwalka KK, Schulze J, Eisele I (2005) Scaling the vertical tunnel FET with tunnel bandgap modulation and gate workfunction engineering. *IEEE Trans. Electron Devices* 52:909–917. https://doi.org/10.1109/TED.2005.846318.
17. Choi WY, Park BG, Lee JD, Liu TJK (2007) Tunneling field-effect transistors (TFETs) with subthreshold swing (SS) less than 60 mV/dec. *IEEE Electron Device Lett* 28:743–745. https://doi.org/10.1109/LED.2007.901273.
18. International Technology Roadmap for Semiconductors. *Semiconductor Industry Association*, 2005.
19. Hraziia VA, Amara A, Anghel C (2012) An analysis on the ambipolar current in SI double-gate tunnel FETs. *Solid-State Electron* 70: 67–72. https://doi.org/10.1016/j.sse.2011.11.009
20. Sze SM, Ng KK (2007) Physics of Semiconductor Devices. Hoboken. NJ, USA: Wiley 315.
21. Kanungo S, Chattopadhyay S, Gupta PS, Rahaman H (2015) Comparative performance analysis of the dielectrically modulated fullgate and short-gate tunnel FET-based biosensors. *IEEE Trans. Electron Devices* 62:994–1001. https://doi.org/110.1109/TED.2015.2390774
22. Narang R, Saxena M, Gupta M (2015) Comparative analysis of dielectric-modulated FET and TFET-based biosensor. *IEEE Trans Nanotechnol* 14:427–435.https://doi.org/110.1109/TNANO.2015-.2396899

23. Leung, Greg, Chui CO (2012) Variability impact of random dopant fluctuation on nanoscale junctionless FinFETs. *IEEE Electron Device Lett* 33:767-769. https://doi.org/10.1109/LED.2012.2191931
24. Sahu C, Singh J (2014) Charge-plasma based process variation immune junctionless transistor. *IEEE Electron Device Lett* 35:411–413. https://doi.org/10.1109/LED.2013.2297451
25. Ghosh B, Akram MW (2013) Junctionless tunnel field effect transistor. *IEEE Electron Device Lett* 34:584–586. https://doi.org/10.1109/LED.2013.2253752
26. Venkata B et al (2017) Junctionless based dielectric modulated electrically doped tunnel FET based biosensor for label-free detection. *Micro Nano Lett* 13:452–456. https://doi.org/10.1049/mnl.2017.0580
27. Lahgere A, Sahu Ch, Singh J (2015) PVT-Aware Design of Dopingless Dynamically Configurable Tunnel FET. *IEEE Electron Devices* 62:2404-2409. https://doi.org/10.1109/TED.2015.2446615.
28. Busse S, Scheumann V, Menges B, Mittler S (2002) Sensitivity studies for specific binding reactions using the biotin/streptavidin system by evanescent optical methods.*Biosensors Bioelectron* 17:704–710.https://doi.org/10.1016/S0956-5663(02)00027-1
29. Poghossian A, Cherstvy A, Ingebrandt S, Offenhäusser A, Schöning MJ (2005) Possibilities and limitations of label-free detection of DNA hybridization with field-effect-based devices. *Sens Actuators B,Chem* 111–112:470–480. https://doi.org/10.1016/j.snb.2005.03.083
30. ATLAS Device Simulation Software, Silvaco Int. Santa Clara, CA, USA, 2014. Available: http://www.silvaco.com.
31. Goswami R, Bhowmick B (2019) Comparative analyses of circular gate TFET and heterojunction TFET for dielectric-modulated label free biosensing. *IEEE Sensors J* 19:9600-9609. https://doi.org/10.1109/JSEN.2019.2928182
32. Kannan N, Kumar MJ (2013) Dielectric-modulated impact-ionization MOS transistor as a label-free biosensor. *IEEE Electron Device Lett* 34:1575–1577. https://doi.org/10.1109/LED.2013.2283858
33. Chong C, Liu H, Wang S, Chen S, Xie H (2021) Sensitivity Analysis of Biosensors Based on a Dielectric Modulated L-Shaped Gate Field-Effect Transistor. *Micromachines* 12: 19. https://dx.doi.org/10.3390/mi1201 0019
34. Silveira F, Flandre D, Jespers PGA (1996) A gm/ID based methodology for the design of CMOS analog circuits and its application to the synthesis of a silicon-on-insulator micropower OTA. *IEEE J Solid- State Circuits* 31:1314-1319. https://doi.org/10.1109/4.535416
35. Kim CH et al (2012) A new sensing metric to reduce data fluctuations in a nanogap embedded field-effect transistor biosensor. *IEEE Trans. Electron Devices* 59:2825-2831.doi.org/10.1109/TED.2012.2209650
36. Goswami R, Bhowmick B (2019) Comparative analyses of circular gate TFET and heterojunction TFET for dielectric-modulated label free biosensing. *IEEE Sensors J* 19:9600-9609. doi.org/10.1109/JSEN.2019.2928182
37. Anand S, Singh A, Amin SI, Thool AS (2019) Design and performance analysis of dielectrically modulated doping-less tunnel FET-based label free biosensor. *IEEE Sensors J* 19:4369–4374. https://doi.org/10.1109/JSEN.2019.2900092
38. Wadhwa G, Raj B (2018) Label free detection of biomolecules using charge-plasma-based gate underlap dielectric modulated junctionless TFET. *J Electronics Mater* 47:4683–4693. https://doi.org/10.1007/s11664-018-6343-1
39. Wangkheirakpam VD, Bhowmick B, Pukhrambam PD (2020) N+ pocket doped vertical TFET based dielectric-modulated biosensor considering non-ideal hybridization issue: A simulation study. *IEEE Trans. Nanotech* 19:156–162. https://doi.org/10.1109/TNANO.2020.2969206
40. Mukhopadhyay S, Sen D, Goswami B, Sarkar SK (2021) Performance Evaluation of Dielectrically Modulated Extended Gate Single Cavity InGaAs/Si HTFET Based Label-Free Biosensor Considering Non-Ideal Issues. *IEEE Sensors J* 21:4739 - 4746. https://doi.org/10.1109/JSEN.2020.3033576
41. Patil M, Gedam A, Mishra GP (2021) Performance Assessment of a Cavity on Source Charge Plasma TFET-Based Biosensor. *IEEE Sensors J* 21:2526 - 2532. https://doi.org/10.1109/JSEN.2020.3027031
42. Anam A, Anand S, Amin SI (2020) Design and performance analysis of tunnel field effect transistor with buried strained Si1xGex Source structure based biosensor for sensitivity enhancement. *IEEE Sensors J* 20:13178–13185. https://doi.org/10.1109/JSEN.2020.3004050